

# Internal waves near the buoyancy frequency in a narrow wave-guide

Hans Van Haren\*

Royal Netherlands Institute for Sea Research (NIOZ), P.O. Box 59, 1790 AB Den Burg, The Netherlands

Received 19 November 2003; accepted 17 June 2004

---

## Abstract

High-resolution temperature observations from the northern North Sea were used to study increased isotherm displacement variance above the internal wave spectral continuum near the background buoyancy frequency ( $N$ ). Existing linear WKB-theories attributed such increase to internal reflection at a turning point within a moderately wide wave-guide or to resonant wave generation from outside the wave-guide. In contrast to linear theory and partially following previous suggestions, the present observations showed that in a narrow wave-guide this increase is due to just a few passages of near-monochromatic, mode-1 interfacial waves. Furthermore, it was observed for the first time that these interfacial waves can occasionally grow and increase their frequency ( $\sigma$ ) until  $\sigma = N_B \ll N_{00}$ , where  $N_{00}$  denotes the frequency of the thin interface of thickness  $\Delta z_{00}$  moving up and down and  $N_B$  is the 5-day mean Eulerian background stratification. Maximum-displacement variance reached levels 2 decades above the long-term average value. The maximum-amplitude  $H$  of the  $\sigma \approx N_B$ -waves was half the vertical scale of the mean pycnocline (and inertial shear layer)  $\Delta z_B = 2H$  delineated by depths  $z$  for which  $N(z) \geq N_B$ , the 'wave-guide'. As a result, the high-frequency waves partially determined the background stratification because further growth was not possible, leading to wave breaking at the edges of the wave-guide and thereby decreasing  $N$ . This mechanism for reduction of the pycnocline is different from accepted mechanisms such as boundary mixing and internal mixing following inertial shear. However, as it occurs within a finite thick pycnocline it may be responsible for much of the relatively slow turbulent exchange of nutrients across pycnoclines in shelf seas.

© 2004 Elsevier B.V. All rights reserved.

*Keywords:* Internal waves; Buoyancy frequency; Narrow wave-guide; Northern North Sea; 59 °N, 01 °E

---

## 1. Introduction

The common view is that the seasonal vertical stratification in density inhibits vertical turbulent

exchange of nutrients in shelf seas such as the North Sea, thereby hampering the growth of phytoplankton in summer. This situation is considered to last until autumn storms mix water masses from the weak near-surface and -bottom boundary layers, via turbulence induced by the atmosphere and tidal current friction. Although this boundary mixing is

---

\* Corresponding author.

E-mail address: hansvh@nioz.nl.

important for autumnal pycnocline erosion, recent observations have shown that an internal mixing mechanism can provide turbulent exchange of nutrients in summer (Van Haren et al., 1999), or autumn (Krauss, 1981; Van Haren et al., 2003), whilst the near-surface and near-bottom boundary layers do not overlap until very late in autumn. This internal mixing is generated externally via ‘large-scale’ vertical inertial current shear following a passage of an atmospheric disturbance and creating maximum shear at the pycnocline.

However, as demonstrated in laboratory experiments (Thorpe, 1971) and described theoretically (Turner, 1973), steady shear at the pycnocline does not produce turbulence directly. First, smaller, high-frequency internal waves are generated, which may form overturning billows and eventually break via the large-scale shear and thus produce the diapycnal turbulent mixing, possibly affecting exchange of nutrients. The strength of this mixing across the pycnocline has often been debated. Due to the strong ambient stratification mixing efficiency of the energy input is expected to be only  $\sim 0.25$  (McEwan, 1983), reaching maximum values of  $\sim 0.36$  when the wave amplitude equals the interface thickness as estimated from modelling (Fringer and Street, 2003). Also, wave-induced mixing occurs intermittently,  $\sim 5\%$  of the time (Woods, 1980). So far, there are few oceanographic observations of the relative importance for mixing and the dominant frequency of such small-scale internal waves propagating in stratified seas with or without large external shear.

This paper presents observational evidence from the northern North Sea that enhancement of internal wave energy levels near the buoyancy frequency (the highest possible internal gravity wave frequency, defined below) can be produced by the passage of a few near-monochromatic waves and their association with local stratification. Such high-frequency near-monochromatic (narrow band) waves occurring mainly in the lowest vertical mode in groups of 2–12 waves have been observed previously (Sabinin, 1973; Brekhovskikh et al., 1975). The variability within the group, and thus the variation with time of spectral peaks near the buoyancy frequency, was hypothesised to be connected with the (unspecified) generation mechanism and/or affected by the wave-guide (stratification) variability with time (Brekhov-

skikh et al., 1975). The latter, possibly nonlinear, interaction between wave-guide and wave groups was considered an important mechanism for diapycnal mixing (Shrira, 1981; Miropol’sky, 2001). The observations presented here show many features of the observations above and focus in more detail on some aspects of this interaction, using a specially designed high-resolution thermistor string (Van Haren et al., 2001).

In the ocean interior, internal gravity waves exist at frequencies  $f < \sigma < N$ ,  $N \gg f$ , between the inertial frequency  $f$  at which motions are purely horizontal, and the ‘background, average large-scale,’ buoyancy frequency  $N(z) = (-g \, \text{dln}\rho/\text{d}z)^{0.5}$ , the natural frequency of vertical oscillation in a density ( $\rho$ ) stratified fluid ( $g$  denotes the acceleration of gravity). This definition of  $N$  implies averaging over time and vertical length scales that are much larger than those of internal waves. Strictly speaking, this means averaging over periods much larger than the inertial period, and over vertical scales much larger than the typical inertial shear length scale. This scale  $\Delta z_S \approx 5$  m in the northern North Sea (Van Haren et al., 2003), where the vertical current shear vector is defined as  $\mathbf{S} = (\partial u/\partial z, \partial v/\partial z)$ . Henceforth, as shown in Fig. 1, we define the ‘Eulerian background stratification of the

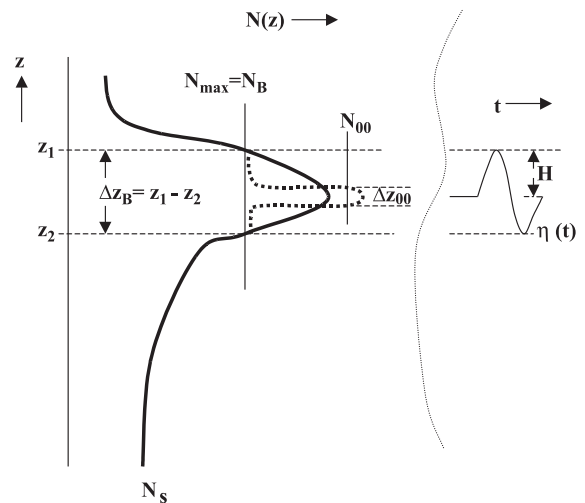


Fig. 1. Definition sketch of stratification, with the thick and dashed extension profiles computed at a vertical resolution of  $\sim 0.1$  m (see text for all definitions).  $N_{\max}$  and  $N_B$  indicate the background Eulerian mean stratification in the pycnocline.  $N_{00}$  indicates ‘local stratification’.

pycnocline' ('stratification' in short)  $N_{\max} = N_B$  as the maximum in a profile of stratification  $N$  when averaged over  $\Delta z_B = 6$  m and  $\Delta t = 5$  d. These averaging scales seem somewhat arbitrarily chosen, but reflect the length and time scales of vertical inertial current shear that is circularly polarised (Van Haren, 2000; Knight et al., 2002; Van Haren et al., 2003). Locally in thin layers and/or for short periods, stratification computed at the resolution of the thermistor string ( $\Delta z = 1$  m,  $\Delta t = 30$  s) may become very large:  $N_{00} \gg N_B$  in Fig. 1. We distinguish near-surface and near-bottom 'well-mixed' layers from layers of 'enhanced stratification' where  $\Delta T/\Delta z > 0.01$  °C m<sup>-1</sup>, that is where average  $N(z) > 10f$ .

Whilst motions near  $f$  generally dominate the destabilising vertical current shear in shelf seas,  $N$  determines stability and energy scaling in the deep-ocean: Garrett and Munk (1972; henceforth GM) derived the scaling  $N^{-1}\sigma^{-2}$  for the average deep-ocean internal gravity wave continuum displacement spectrum (and  $N\sigma^{-2}$  for the average energy spectrum) in the range  $f \ll \sigma \ll N$ . Voorhis (1968), Sabinin (1973), Brekhovskikh et al. (1975), Cairns (1975) and Cairns and Williams (1976) showed that near the buoyancy frequency potential energy (hence also isotherm displacement) spectra were enhanced above this internal wave band continuum. Sabinin (1973) suggested that this enhancement was entirely due to a few passages of high-frequency internal wave groups, whose energy becomes 'hidden' in long-term averages.

Earlier, Sabinin (1966) suggested an explanation for the observed discrepancy between  $N_{\max}$  in a pycnocline and the spectral peak frequency  $N_R = 1.1N_S \ll N_{\max}$  of waves observed between depths  $z_1$  and  $z_2$  (Fig. 1).  $N_S$  is the constant buoyancy frequency of a thick layer well below the pycnocline (Fig. 1). Sabinin suggested that the dominant waves at  $\sigma = N_R$  were generated by an (unspecified) resonance mechanism by motions in the thick layer below. This mechanism is not applicable for our shelf sea, since  $N_S \neq$  constant and dominant motions, having amplitudes  $H$ , within the pycnocline have frequency  $\sigma = N_B \gg N_S$ ,  $N_S \leq 10f \ll N_B$ , as will be shown in Section 3.

To model the observed spectral enhancement near  $N$  Desaubies (1973) introduced Airy functions and Desaubies (1975) suggested a maximum vertical

mode-number of  $j = 10$ – $15$ , ~half the number originally suggested by GM. However, this theoretical enhancement was more peaked near  $N$  than the observations. Cairns (1975) suggested the use of less modes  $j \approx 5$ , which was used in follow-up GM-models (Garrett and Munk, 1975 and subsequent). A better correspondence between theory and ocean observations was obtained by Munk (1980), who argued that the wave-guide had to be sufficiently wide (with the vertical scale of the pycnocline  $\gg$  the amplitude of the waves of  $\sigma \ll N_{\max}$ ), so that the physical explanation was valid of 'soft'-reflecting high-frequency internal waves (that is reflection without energy loss at their 'turning point' in the vertical). Despite its validity in a WKB sense and its success in describing average internal wave spectra near the buoyancy frequency, Munk's (1980) argument does not hold for a shelf sea, which is under wind- and bottom friction stress, just like Sabinin's (1966) suggestion. In a shelf sea under turbulent boundary layer stress the wave-guide may become very narrow (with the vertical scale of the pycnocline  $\approx$  the amplitude of the waves; but not necessarily equal to the interface thickness as in Fringer and Street, 2003), for example due to erosion from above and below or due to a sudden change in near-inertial shear across the stratification (Linden, 1979; Van Haren and Howarth, 2004). Its effect on high-frequency internal waves is shown in this paper.

## 2. Data

A specially designed thermistor string was moored in the northern North Sea at 59° 19.05' N, 01° 00.52' E, 110 m water depth, for nearly two weeks in late October during autumnal decrease in stratification. The thermistor string held 32 sensors evenly spaced at 1 m intervals. The sensors had a relative accuracy better than 0.5 mK, they had a response time better than 0.25 s, they were all sampled within 4 s and data were stored once every 30 s (further details in Van Haren et al., 2001). The temperature data  $T(z,t)$  were converted to vertical displacements  $\eta(T,t)$  of isotherms, from which displacement spectra  $P_{\eta}(\sigma)$  were computed. In contrast to Eulerian temperature spectra, such

displacement spectra do not suffer from ‘fine-structure contamination’ (Pinkel, 1981). During the first week of deployment CTD information was obtained to determine the location of the entire pycnocline and to establish a relationship  $\delta\rho = -(0.25 \pm 0.01)\delta T$ . During the deployment period the near-surface temperature dropped from  $10.4 \rightarrow 9.2$  °C (Knight et al., 2002; Van Haren et al., 2003). The near-bottom temperature also decreased with time, but only by  $0.02$  °C around  $7.4$  °C, implying no direct evidence for mixing across the entire pycnocline.

### 3. Observations

#### 3.1. General stratification variations

The 13-d period of observations showed distinct variation in pycnocline stratification, termed  $N_A$ ,  $N_B$ ,  $N_{00}$ . Within a week of deployment, the high-frequency enhancement in the displacement spectrum shifted to lower frequencies by about half a decade ( $N = N_A \rightarrow N_B$ ; Fig. 2a). Meanwhile, its spectral level increased by the factor  $(N_B/N_A)^{-1} = 2.25$  at frequencies well within the internal wave band ( $5 < \sigma < 50$  cpd),

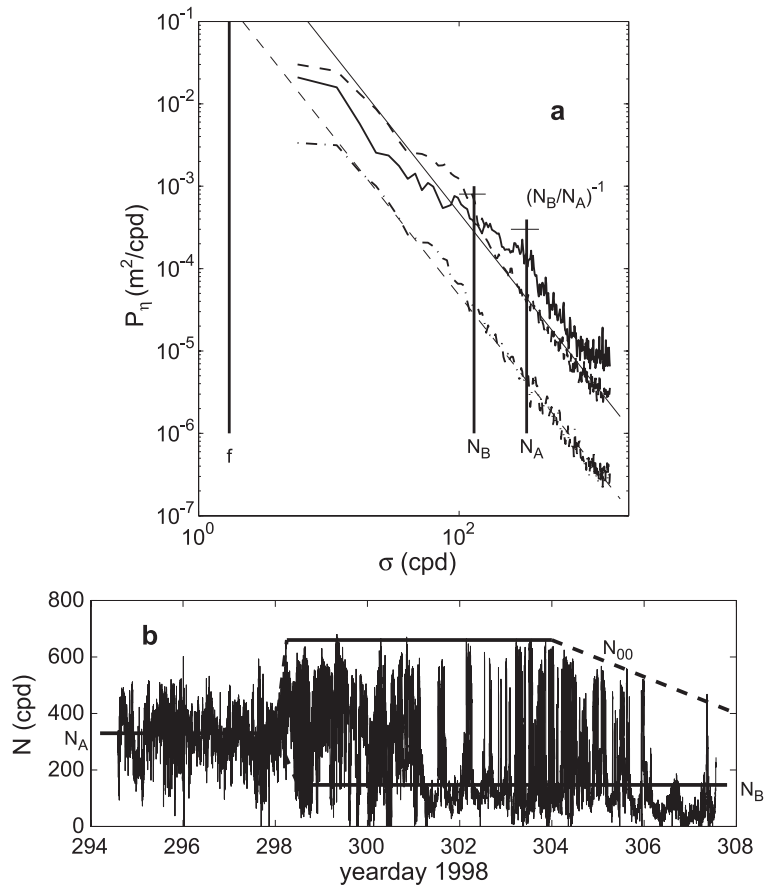


Fig. 2. (a) Observed spectra  $P_\eta(\sigma)$ , which were computed for different 5-d periods using  $7.600$  °C-isotherm data interpolated from thermistor string data. The solid spectrum represents days 294.6–299.6 ( $N_{\max} = N_A$ ), the dashed spectrum 300.5–305.5 ( $N_{\max} = N_B$ ). The dash-dotted spectrum offset by 1 decade is the average over days 300.5–303.5 and 304.5–306.5. One standard deviation of buoyancy frequency is indicated by horizontal lines on top of both solid vertical lines, which indicate the central frequencies. The height difference of these vertical lines indicates the factor  $(N_B/N_A)^{-1}$ . The sloping lines indicate the GM continuum spectral slope of  $\sigma^{-2}$ . (b) Time series of buoyancy frequency computed every 30 s around  $z = -60$  m from two neighbouring thermistors.  $N_A$  and  $N_B$  are as in a,  $N_{00}$  indicates the short-term buoyancy frequency in thin layers passing the sensors occasionally.

in accordance with GM. As was shown by Van Haren and Howarth (2004), the transition to large-scale (~5 m vertically, ~5 days in time) stratification followed after a sudden drop in near-inertial current shear across the pycnocline on day 298, with new equilibria established by day 300. The drop in near-inertial current shear came after the passage of a storm, apparently with currents generated by wind-stress being 180° out-of-phase with existent near-inertial motions near the surface (Knight et al., 2002). The second period (B)

also showed very stable stratification  $N_{00} \gg N_B$  in a thin layer  $\Delta z_{00} \approx 1$  m (Van Haren and Howarth, 2004), so that  $N_A \rightarrow N_B, N_{00}$  (Fig. 2b). The  $N_{00}$  was observed over short periods (minutes) in a Eulerian frame of reference (Figs. 2b and 3e), and over long periods of several days in an isotherm-following frame of reference.

In all three cases of different stratification of the pycnocline  $N_A$  (with strong inertial shear),  $N_B$  (with weak shear) and  $N_{00}$  (very thin interface), the

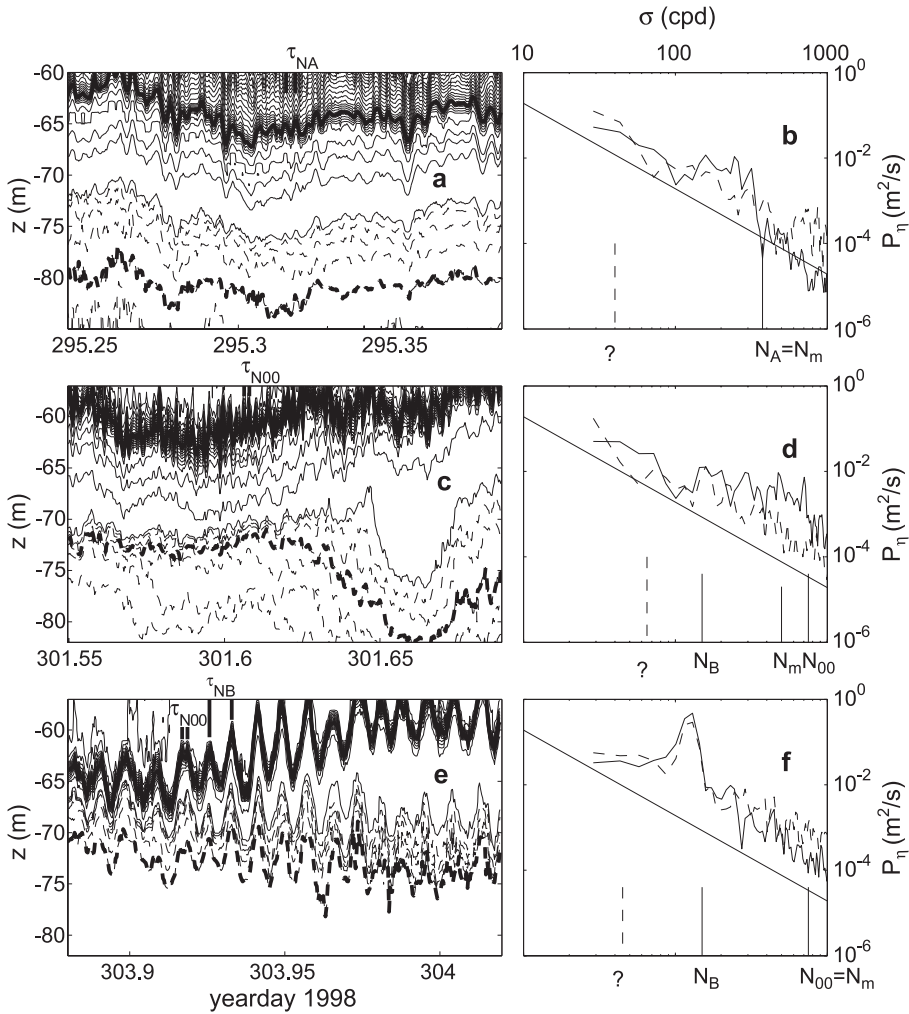


Fig. 3. (a, c, e) Isotherm displacements with time for three typical 0.14-d periods with different stratification. Solid contours are drawn every 0.1 °C for [7.5, 9.8] °C, dashed contours are drawn every 0.01 °C. Representative waves are indicated having periods  $\tau_{NA}, \tau_{NB}, \tau_{N00}$ . In b, d and f nearly raw ( $\nu \approx 3$  degrees of freedom, df) displacement spectra are shown for the heavy, solid and dashed isotherms in a, c and e, respectively.  $N_m$  and question mark ? indicate 0.14-d averaged local stratification computed in isotherm following coordinates for heavy, solid and dashed isotherms, respectively.  $N_{00}$  indicates the largest local stratification. Five-day mean background Eulerian stratification of the pycnocline is indicated by  $N_A$  (between  $-66 < z < -60$  m),  $N_B$  (between  $-68 < z < -62$  m).

enhancement in displacement spectra near these frequencies was due to a few bursts of small temporal scale waves occurring in  $\sim 10\text{--}20\%$  of the observations (Fig. 3), as described by Sabinin (1973). For example, the overall spectral enhancement above the mean spectral slope near  $N_B$  was entirely attributable to a one-day burst of the high-frequency internal waves (Fig. 3e and f). Also note the dashed spectrum in Fig. 3f in relation to the estimated (question mark) local buoyancy frequency: evidence of evanescent waves associated with the free waves in the ( $N_B > N_?$ ) pycnocline. Otherwise over the 5-d period the spectrum was continuous across  $N_B$  (the off-set spectrum in Fig. 2a). This spectral continuation for  $\sigma > N_B$  was due to the thin layer stratification observed here (Fig. 3e): very high-frequency ( $N_B < \sigma < N_{00}$ ) internal waves occurred in small groups in a very thin layer that was moved occasionally past the sensors by lower frequency ( $\sigma \leq N_B$ ) internal waves. Such passages were shorter than 0.14 d (the averaging interval in Fig. 3), hence an example of measured  $N_m = N_{00}$  enhancement cannot be given; Fig. 3c and d is a ‘reasonable example’. The existence of these very high-frequency internal waves prevented the observation of 5-d mean displacement spectra that fell off sharply near  $N_B$ .

### 3.2. Detail of wave growth filling a wave-guide

The spectrum averaged over the one day 303.5–304.5 (not shown) demonstrated a local minimum below the canonical internal wave continuum GM level at  $f \ll \sigma \ll N_B$  which was as large as the enhancement above this continuum near  $\sigma \approx N_B$ . Around day 303.5 this energy enhancement commenced at  $\sigma < N_B$  (Fig. 4). With time, spectra were computed for 0.14 d data pieces in steps of 0.07 d, amplitude and frequency increased up to their maximum values at day 303.95, the maximum frequency being at the background Eulerian buoyancy frequency of the pycnocline ( $N_B$ ), established at day 297.8. The maximum spectral amplitude extended two decades above the  $\sigma^{-2}$ -slope. During the growth stage the extent above the GM continuum level occupied more or less the same frequency band, whilst bandwidth  $\Delta\sigma$  between frequency limits where  $P(\sigma) = \pm 0.1P(\sigma_p)$  around the peak frequency  $\sigma_p$  decreased to its minimum at day 303.95, when the maximum

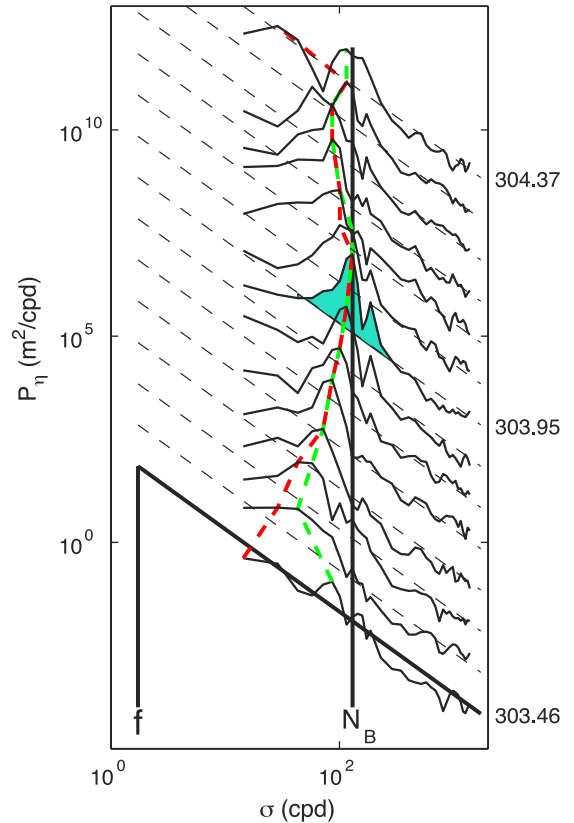


Fig. 4. Displacement spectra of 0.14-d data pieces of the 7.600 °C isotherm, off-set in time by 0.07 d and one decade in energy. With each spectrum, a  $\sigma^{-2}$ -slope is indicated for reference. A few central timestamps are indicated on the right-hand vertical axis. The red dashed line follows the peak value in each of the spectra, which increases with time while shifting towards higher frequencies. The nearly identical green dashed line follows peaks with respect to the  $\sigma^{-2}$ -slopes.

amplitude was reached. The maximum amplitudes and frequencies of the  $N_B$ -waves lasted less than 1.5 h, that is less than 10 buoyancy periods  $\tau_{NB}$  (Fig. 5).

During this relatively short period of time, the waves were close to monochromatic and thus not so widely smeared in frequency as average spectra suggested. The length of the wave-group pointed to a relative bandwidth  $\Delta\sigma/\sigma_p \approx 0.1$ . This value was similar to that observed for internal near-inertial and tidal bandwidths in the deep ocean (Van Haren, 2004). The vertical limitation of growth of  $N_B$ -waves was apparent from the red curves in Fig. 5, where the maximum wave excursion  $2H$  just fitted the wave-guide set by the limits of  $N_B$ :  $2H = \Delta Z_B$  (between the

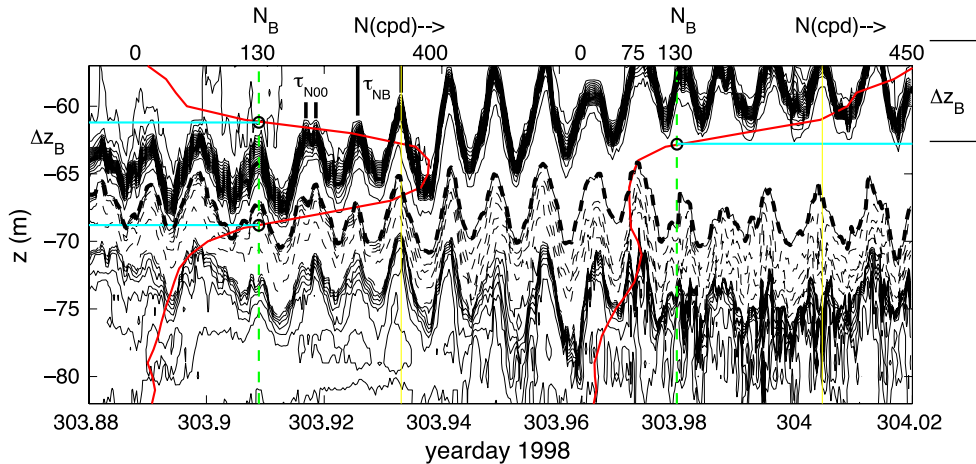


Fig. 5. As Fig. 3e but including contours every  $0.001\text{ }^{\circ}\text{C}$  (lower solid contours) and estimates of the wave-guide widths  $\Delta z_B$  for  $\sigma \leq N_B$  (between the blue lines delineated by the red curves and the green dashed lines). The red curves indicate Eulerian  $N(z)$  (axes on top), which was computed twice using averages over  $\Delta z = 1\text{ m}$  and  $\Delta t = 0.03\text{ d}$  around the position of the green vertical dashed lines at 5-d mean background Eulerian  $N_B = 130\text{ cpd}$  (the solid  $N$  graph in Fig. 1 resembles the red curves). The depth intervals between intersections of these vertical dashed lines and the red curves, between o-o for the first red curve and above -o for the second, indicate the depths where  $N(z) > N_B$ . The vertical yellow lines are for referencing wave crests at various depths.

blue lines). The waves occurred with a mode  $j = 1$  structure as observed before (Sabinin, 1973; Brekhovskikh et al., 1975; Eriksen, 1978), closely following the wave-guide strained by some lower-frequency differential advection and near-surface and near-bottom mixing. Occasionally, these waves carried higher frequency waves ( $\sigma \approx N_{00}$ ), not only at crests as indicated but also on the flanks of the  $N_B$ -waves. Such high  $N$ -values were not found by computing the 0.03-d Eulerian mean, showing that such an averaging period is too long to find  $N_{00}$  (cf. the 30 s intervals used in computing  $N$  in Fig. 2b). Although the values of all background Eulerian pycnocline stratification  $N_{\max}$  were dominated by averaging a few passages of  $N_{\max}$ -waves displacing thin layers of stronger stratification, e.g. also the examples in Fig. 3a and b, only the  $N_{00}$ -waves and the one event in Fig. 5 filled the wave-guide. The latter was the most dramatic and pronounced, evidence of highly non-linear generation as it appeared in a (wave-)group that cannot be described using linear theory, despite the apparent highly linear shape of individual waves.

Until day 303.92, the entire layer of enhanced stratification ( $N > 10f$ ) was restricted between  $-76 < z < -62\text{ m}$  by boundary mixing, as evidenced from the irregular contours above and below the regular waves. The very strong stratification ( $N_{00}$ ) was

maintained for six days, until day  $\sim 304$  (Fig. 2b), after which this thin-layer stratification was gradually reduced mainly by a thickening of its layer together with a relaxation of boundary mixing. Around this date wind stress was negligible (Van Haren and Howarth, 2004). This reduction in  $N_{00}$  followed the period of maximum amplitude of the large  $N_B$ -waves that were also found outside the wave-guide, albeit having lesser amplitudes, probably ‘evanescent waves’. The lower ‘pycnocline’ had a local buoyancy frequency of only  $\sim 0.6N_B$ , decreasing with time. After day 303.95, when maximum amplitude at frequency  $N_B$  was reached, the latter waves were accompanied by observed overturns, as evidenced from the irregular and closed contours, notably in the dashed wave contours between  $\sim 70$  and  $75\text{ m}$  depth. This suggested mixing by wave breaking (in addition to boundary mixing) outside the edges of the wave-guide, mainly below the pycnocline. This eventually resulted in an overall reduction of background Eulerian stratification  $<N_B$  from day 305.5 onward (Fig. 2b).

#### 4. Discussion

Changes in stratification commonly influence high-frequency waves. A new aspect was shown in the

present observations in which high-frequency internal gravity waves may grow up to the layer thickness of their wave-guide before dissipating. As a result, they can influence overall internal wave scaling by reduction of Eulerian background stratification. Obviously, such high-frequency waves should eventually break under enhanced (near-inertial) shear (Marmorino, 1987; Marmorino et al., 1987), like evanescent waves observed at the edges of stratification by Eriksen (1978) and in the present paper (lower right half in Fig. 5). Woods (1980) postulated that ‘sheet waves’, short waves trapped in thin sheets of enhanced static stability, are the most important waves breaking in the ocean. Woods suggested that such ‘breaking’ waves result from interaction of thin layers of stratification (finestructure) and free internal waves. In terms of the previous observations, this would mean motions at  $\sigma > N$  (for large-scale  $N$ ) breaking, advected by motions at  $f < \sigma < N$ . This is observed (Fig. 5), although the ‘breaking wave motions’ seem more evanescent waves, as suggested by Eriksen (1978). The intermittency of their breaking may reflect a state of continual re-attainment of dynamical instability (Woods, 1980), or a near-critical value of the gradient Richardson number. The latter was observed in the northern North Sea for all three situations  $N_A$ ,  $N_B$  and  $N_{00}$  (Van Haren and Howarth, 2004).

It is not possible to conclude from the present observations where the energy supply for the high-frequency internal waves originated. The observations suggest that the mechanism for growth of near  $N$ -waves relied on the input from the atmosphere through the sea surface, as was suggested from the downward propagation of wave energy inferred from forward slanted wave crests with respect to yellow vertical lines in Fig. 5, indicative of upward phase propagation (Thorpe, 1987). Curiously, around their time of generation wind stress dropped from moderate to weak (Van Haren and Howarth, 2004). Also, near-inertial shear was weak. Evidence for wave-wave interaction is lacking, as surface wave data were not available and tidal (higher) harmonics are unlikely to generate such infrequently occurring  $N$ -waves.

Although the presented observations of occasional wave growth just filling its wave-guide and entirely dominating the above-GM spectral enhancement near

$N$  are from shelf seas, this may be observed in the deep ocean as well. The link is through variations in near-inertial motions that are important for internal wave shear and thickness variation of enhanced stratification. In the deep ocean pycnocline thickness variations with time or straining are not likely to be caused by external stresses as in the North Sea, but are brought about inside the internal wave field itself (Pinkel, 1981). The mode-1 motions near  $(f, N)$  are important for motions at other internal wave frequencies, which may occur in different higher modes given the observed GM-scaling. It is suggested that future ocean studies focus on the variations of motions near both edges  $(f, N)$  of the internal wave frequency band in spectra, also to establish variability in ocean mixing. It remains to be established whether the observed same number of waves in groups (same relative bandwidth) at  $f$  and  $N$  is coincidental or whether it has some relationship with mixing induced by internal waves. The occasional breaking of these high-frequency waves, whether or not supported by large-scale shear, seems dominant in vertical exchange of nutrients (with estimated eddy diffusivity values of  $0.3 \times 10^{-4} \text{ m}^2 \text{ s}^{-1}$  in summer (Van Haren et al., 1999) and  $3 \times 10^{-4} \text{ m}^2 \text{ s}^{-1}$  in autumn (Van Haren et al., 2003)). As a result, they are important for phytoplankton late-summer/autumn blooms. In the present paper, the evidence of localised mixing, as inferred from closed contours in the high-resolution temperature data, proves that turbulence exists in strongly stratified layers. In future studies, the above spectral studies may prove a useful addition to direct measurements of  $N(z)$ , which remain difficult using CTD and moored instruments due to uncertainties in suitable averaging scales.

### Acknowledgements

I enjoyed the assistance of the crew of RV ‘Pelagia’. I highly appreciated discussions with Ruud Groenewegen and Martin Laan on the NIOZ Fast Thermistor String. Theo Hillebrand helped prepare and deploy the instruments during PROVESS, a MAST3 project funded in part by the Commission of the European Communities Directorate General for Science and Education, Research and Development under contract #MAS3-CT97-0159.

## References

- Brekhovskikh, L.M., Konjaev, K.V., Sabinin, K.D., Serikov, A.N., 1975. Short-period internal waves in the sea. *J. Geophys. Res.* 80, 856–864.
- Cairns, J.L., 1975. Internal wave measurements from a mid-water float. *J. Geophys. Res.* 80, 299–306.
- Cairns, J.L., Williams, G.O., 1976. Internal wave observations from a mid-water float, II. *J. Geophys. Res.* 81, 1943–1950.
- Desaubies, Y.J.F., 1973. Internal waves near the turning point. *Geophys. Fluid Dyn.* 5, 143–154.
- Desaubies, Y.J.F., 1975. A linear theory of internal wave spectra and coherences near the Väisälä frequency. *J. Geophys. Res.* 80, 895–899.
- Eriksen, C.C., 1978. Measurements and models of fine structure, internal gravity waves, and wave breaking in the deep ocean. *J. Geophys. Res.* 83, 2989–3009.
- Fringer, O.B., Street, R.L., 2003. The dynamics of breaking progressive interfacial waves. *J. Fluid Dyn.* 494, 319–353.
- Garrett, C.J.R., Munk, W.H., 1972. Space-time scales of internal waves. *Geophys. Fluid Dyn.* 3, 225–264.
- Garrett, C., Munk, W., 1975. Space-time scales of internal waves: a progress report. *J. Geophys. Res.* 3, 291–297.
- Knight, P.J., Howarth, M.J., Rippeth, T., 2002. Inertial currents in the northern North Sea. *J. Sea Res.* 47, 269–284.
- Krauss, W., 1981. The erosion of the pycnocline. *J. Phys. Oceanogr.* 11, 415–433.
- Linden, P.F., 1979. Mixing in stratified fluids. *Geophys. Astrophys. Fluid Dyn.* 13, 3–23.
- Marmorino, G.O., 1987. Observations of small-scale mixing processes in the seasonal thermocline Part II: wave breaking. *J. Phys. Oceanogr.* 17, 1348–1355.
- Marmorino, G.O., Rosenblum, L.J., Trump, C.L., 1987. Fine-scale temperature variability: the influence of near-inertial waves. *J. Geophys. Res.* 92, 13,049–13,062.
- McEwan, A.D., 1983. The kinematics of stratified mixing through internal wavebreaking. *J. Fluid Mech.* 128, 47–57.
- Miropol'sky, Yu.Z., 2001. *Dynamics of Internal Gravity Waves in the Ocean*. Kluwer Academic Publishers Dordrecht, Netherlands. 406 pp.
- Munk, W.H., 1980. Internal wave spectra at the buoyant and inertial frequencies. *J. Phys. Oceanogr.* 10, 1718–1728.
- Pinkel, R., 1981. Observations of the near-surface internal wave field. *J. Phys. Oceanogr.* 11, 1248–1257.
- Sabinin, K.D., 1966. Connection of short-period internal waves with the vertical density gradient in the sea. *Izv. Acad. Sci. USSR Atmos. Ocean. Phys.* 2, 872–882.
- Sabinin, K.D., 1973. Certain features of short-period internal waves in the ocean, 1973. *Izv. Acad. Sci. USSR Atmos. Ocean. Phys.* 9, 32–36.
- Shrira, V.I., 1981. On the propagation of a three-dimensional packet of weakly non-linear internal gravity waves, 1981. *Int. J. Non-linear Mech.* 16, 129–138.
- Thorpe, S.A., 1971. Experiments on the instability of stratified shear flows: miscible fluids. *J. Fluid Mech.* 46, 299–319.
- Thorpe, S.A., 1987. Current and temperature variability on the continental slope. *Phil. Trans. Roy. Soc. Lond.* A323, 471–517.
- Turner, J.S., 1973. *Buoyancy Effects in Fluids*. Cambridge University Press, Cambridge. 368 pp.
- Van Haren, H., 2000. Properties of vertical current shear across stratification in the North Sea. *J. Mar. Res.* 58, 465–491.
- Van Haren, H., 2004. Bandwidth similarity at inertial and tidal frequencies in kinetic energy spectra from the Bay of Biscay. *Deep-Sea Res.* I 51, 637–652.
- Van Haren, H., Howarth, M.J., 2004. Enhanced stability during reduction of stratification in the North Sea. *Cont. Shelf Res.* 24, 805–819.
- Van Haren, H., Maas, L., Zimmerman, J.T.F., Ridderinkhof, H., Malschaert, H., 1999. Strong inertial currents and marginal internal wave stability in the central North Sea. *Geophys. Res. Lett.* 26, 2993–2996.
- Van Haren, H., Groenewegen, R., Laan, M., Koster, B., 2001. A fast and accurate thermistor string. *J. Atmos. Oceanic Technol.* 18, 256–265.
- Van Haren, H., Howarth, M.J., Jones, K., Ezzi, I., 2003. Autumnal reduction of stratification in the northern North Sea and its impact. *Cont. Shelf Res.* 23, 177–191.
- Voorhis, A.D., 1968. Measurements of vertical motion and the partition of energy in the New England slope water. *Deep-Sea Res.* 15, 599–608.
- Woods, J.D., 1980. Do waves limit turbulent diffusion in the ocean? *Nature* 288, 219–224.